Structural Characterization of Cardiolipin by Tandem Quadrupole and Multiple-Stage Quadrupole Ion-Trap Mass Spectrometry with Electrospray Ionization

Fong-Fu Hsu and John Turk
Mass Spectrometry Resource, Division of Endocrinology, Diabetes, Metabolism, and Lipid Research, Department of Internal Medicine, Washington University School of Medicine, St. Louis, Missouri, USA

Elizabeth R. Rhoades and David G. Russell
Department of Microbiology and Immunology, Cornell University, Ithaca, New York, USA

Yixin Shi and Eduardo A. Groisman
Department of Molecular Microbiology, Washington University School of Medicine, St. Louis, Missouri, USA

We report negative-ion electrospray tandem mass spectrometric methods for structural characterization of cardiolipin (CL), a four-acyl-chain phospholipid containing two distinct phosphatidyl moieties, of which structural assignment of the fatty acid residues attached to the glycerol backbones performed by low-energy CAD tandem mass spectrometry has not been previously described. The low-energy MS^2-spectra of the $[M - H]^-$ and $[M - 2H]^{2-}$ ions obtained with ion-trap or with tandem quadrupole instrument combined with ion-trap MS^3-spectra or with source CAD product-ion spectra provide complete structural information for CL characterization. The MS^2-spectra of the $[M - H]^-$ ions contain two sets of prominent fragment ions that comprise a phosphatidic acid, a dehydrated phosphatidylglycerol, and a (phosphatidic acid + 136) anion. The substantial differences in the abundances of the two distinct phosphatidic anions observed in the MS^2-spectra of the $[M - H]^-$ ions lead to the assignment of the phosphatidyl moieties attached to the 1′ or 3′ position of central glycerol. Upon further collisional dissociation, the MS^3-spectra of the phosphatidic anions provide information to identify the fatty acyl substituents and their position in the glycerol backbone. The MS^2-spectra of the $[M - 2H]^{2-}$ ions obtained with TSQ or ITMS contain complementary information to confirm structural assignment. The applications of the above methods in the differentiation of cardiolipin isomers and in the identification of complex cardiolipin species consisting of multiple molecular structures are also demonstrated. (J Am Soc Mass Spectrom 2004, 16, 491–504) © 2004 American Society for Mass Spectrometry

Cardiolipin (CL) (**I**) contains a phosphatidylglycerol that is linked to the phosphoglyceride skeleton to make it a 1,3-bisphosphatidyl-*sn*-glycerol [1, 2]. The compound was first isolated by Pangborn [3]. The trivial name "cardiolipin" is derived from the fact that it was first found in animal hearts, where it is especially abundant and mostly confined to the mitochondria, comprising more than 10% of the total phospholipids of that organ. It can also be found in mitochondria of all animal tissues and of the eukaryotic kingdom [4].

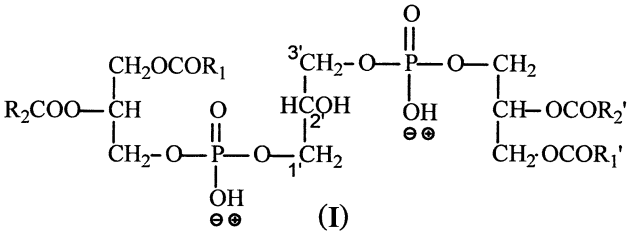

(**I**)

Cardiolipin is essential for the function of several enzymes of oxidative phosphorylation, and thus, for production of energy for the heart to beat [5, 6]. A direct relationship between CL loss and cytochrome *c* release from the mitochondria has been identified as an initial step in the pathway to apoptosis [7, 8]. An absolute requirement for CL in the function of crucial mitochon-

Published online February 24, 2005

Address reprint requests to Dr. F.-F. Hsu, Department of Internal Medicine, Washington University School of Medicine, 660 S. Euclid, Box 8127, St. Louis, MO 63110, USA. E-mail: fhsu@im.wustl.edu

1044-0305/04/$30.00
doi:10.1016/j.jasms.2004.12.015

Received August 2, 2004
Revised December 28, 2004
Accepted December 29, 2004

drial proteins, e.g., cytochrome oxidase and the adenine nucleotide translocase, are likely additional factors impacting apoptosis and cellular energy homeostasis [5–9]. Other potential clinical manifestations of perturbations of CL synthesis are associated with, for instance, Barth Syndrome, where a primary defect can be attributed to CL metabolism and is associated with dilated cardiomyopathy [10, 11]. The regulatory properties that govern CL biosynthesis, its remodeling, and trafficking are beginning to emerge [5–9, 12].

Two pathways are involved in the synthesis of cardiolipin. In the prokaryotic biosynthesis pathway, two molecules of phosphatidylglycerol were involved. In contrast, cardiolipin was synthesized from CDP-diacylglycerol and phosphatidylglycerol in the common eukaryotic mechanism [12–14]. The gross structures of the major cardiolipin species from different sources are very similar. For example, the molecular species of cardiolipin from rat liver, bovine heart, *S. cerevisiae* and *N. crassa* contained mainly 16:0 or 18:2 fatty acid, resulting in a relatively homogeneous distribution of double bonds and carbon numbers among the four acyl positions [14, 15].

The complexities of the molecular species of cardiolipin stem not only from the diversity of different chain lengths for fatty acids and the fatty acids with varying degrees of unsaturation, but also from permutations of the four fatty acyl chains that result in a large number of potential combinations. Thus, unraveling the structure of cardiolipin has been a very difficult task and has been previously approached by a rather complicated method that requires analysis of the total fatty acyl patterns and the positional distribution of acyl chains between *sn*-1 and *sn*-2 positions, analysis of diacyl species of the 1′-phosphatidyl and 3′-phosphatidyl moieties and the resolution of tetraacyl species of derivatized cardiolipin. This approach in the analysis of CL has been mainly conducted by high-performance liquid chromatographic separation of its 1,3-bisphosphatidyl-2-benzoyl-*sn*-glycerol dimethyl ester derivative, followed by characterization of the derivatives involving ^{1}H nuclear magnetic resonance spectroscopy, ultraviolet (uv) spectroscopy, thin-layer chromatography, and fatty acid analysis [15, 16].

ESI with tandem mass spectrometric methods including tandem quadrupole [10], quadrupole-time of flight (Q-TOF) [17], and ion-trap [18] instruments have been attempted for characterization of cardiolipin and glucosylcardiolipin, and result in identifying but not locating the fatty acyl substituents on the glycerol backbone. The subclasses of cardiolipin of glucosyl-, alanyl-, and lysocardiolipins also have been previously characterized by FAB-sector mass spectrometric method, but the structural detail including position of the fatty acyl substituents on the glycerol backbone cannot be determined [19]. Herein, we present tandem mass spectrometric methods using both a triple quadrupole and a quadrupole ion-trap mass spectrometer to characterize cardiolipins isolated from various biological sources. Structures of regio- and configuration isomers of cardiolipin molecules are revealed in details.

Materials and Methods

Isolation of Cardiolipins

Cardiolipin from bovine heart and bis-(1,2-dimyristory-*sn*-glycero-3-phosphoryl)-1′,3′-*sn*-glycerol [(14:0/14:0) (14:0/14:0)-CL] standard were purchased from Avanti Polar Lipid (Alabaster, AL). Cardiolipins from bacterium *Salmonella typhimurium* and from *Mycobacterium bovis* BCG were isolated using the procedures as previously described [20, 21].

Mass Spectrometry

Low-energy CAD tandem mass spectrometry experiments were conducted on a Finnigan (San Jose, CA) TSQ 7000 mass spectrometer equipped with ICIS data system or on a LCQ DECA ion-trap mass spectrometer (ITMS) with X-calibur operation system. Extracts containing cardiolipin (10 to 50 pmol/μL) in methanol/chloroform solution (vol/vol, 1/1) were continuously infused (1 uL/min) to the ESI source, where the skimmer was set at ground potential, the electrospray needle was at 4.5 kV, and temperature of the heated capillary was at 260 °C. This gives both $[M - H]^-$ and $[M - 2H]^{2-}$ ions in the negative-ion mode. For product-ion spectra obtained with a triple stage quadrupole (TSQ) instrument, the precursor ions were selected in the first quadrupole (Q1), collided with Ar (2.3 mTorr) in the rf-only second quadrupole (Q2), and analyzed in the third quadrupole (Q3). The collision energies were set at 22 to 24 eV for the $[M - 2H]^{2-}$ ions and at 46 to 50 eV for the $[M - H]^-$ ions. Both Q1 and Q3 were tuned to unit mass resolution and scanned at a rate of 3 sec/scan. The mass spectra were accumulated in the profile mode, typically for 5 to 10 min for a tandem mass spectrum. For CAD tandem mass spectra obtained with a quadrupole ion-trap instrument, the automatic gain control of the ion trap was set to 5×10^7, with a maximum injection time of 400 ms. Helium was used as the buffer and collision gas at a pressure of 1×10^{-3} mbar. MS^n experiments were carried out with a relative collision energy ranged from 30 to 35% and with an activation q value, with which the desired mass range for the product-ion scan can be set. The activation time was set at 100 ms. The mass resolution was 0.6 Da at half peak height throughout the acquired mass range.

Results and Discussion

Cardiolipin possesses two phosphate charge sites, and forms both $[M - H]^-$ and $[M - 2H]^{2-}$ ions when being subjected to ESI in the negative-ion mode. Beckedorf et al. [17] reported that $[M - 2H + Na]^-$ and $[M - 3H + Na]^{2-}$ ions are the major ions observed for D-glucopyranosylcardiolipin using Q-TOF instrument equipped

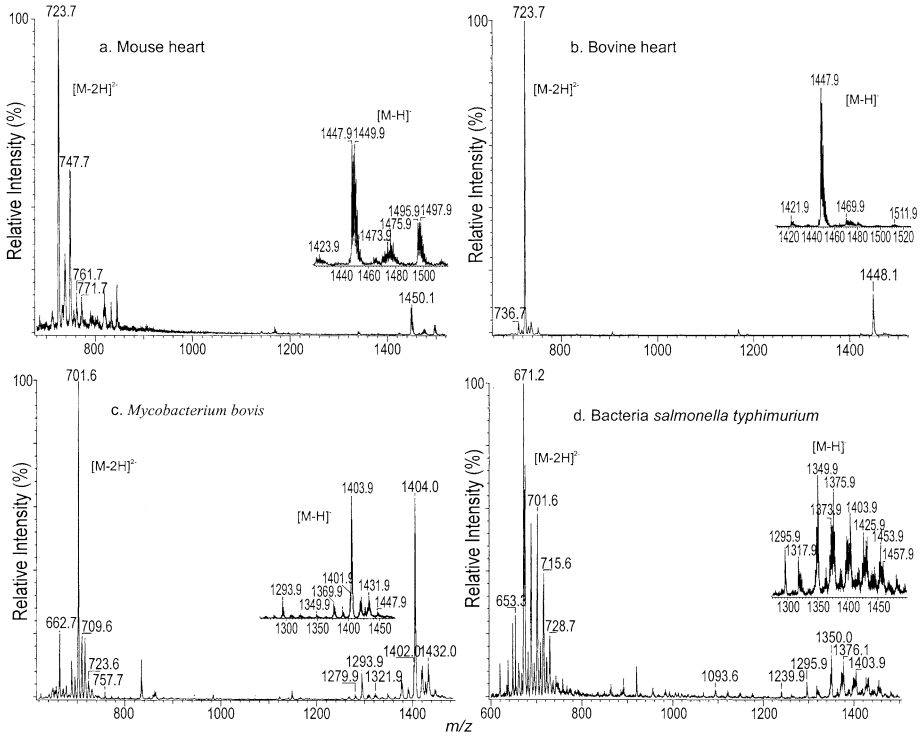

Figure 1. The ESI/MS spectra of cardiolipin mixture isolated from mouse heart (**a**), bovine heart (**b**), *Mycobacterium bovis* (**c**), and bacterium *Salmonella typhimurium* (**d**) obtained with a TSQ instrument.

with a nanospray source, and the $[M - 2H + 3Na]^+$ ions with lesser sensitivity were also observed in the positive-ion mode. However, these ions were not observed in our study, probably attributable to the fact that our CL extracts contained less Na^+. This was achieved by dissolving the sample in 50% methanol (with 0.01 % NH_4OH), followed by extraction with chloroform. This clean-up step also resulted in two to three time increases in the detection of $[M - H]^-$ and $[M - 2H]^{2-}$ ions, with the latter ion is three times more abundant° than° the° former.° Figure° 1° illustrates° the ESI/MS profiles of the cardiolipins isolated from mouse heart (Panel a), bovine heart (Panel b), *Mycobacterium bovis* BCG (Panel c), and bacterium *Salmonella typhimurium* (Panel d) obtained with a TSQ instrument. The spectra demonstrate the diversities of cardiolipin of biological origins, and are similar to those obtained with an ITMS instrument (data not shown). The spectra contain homologous $[M - H]^-$ ions and the $[M - 2H]^{2-}$ species. Structural characterizations of the individual molecular species are described below.

The Fragmentation Processes Revealed by Tandem Quadrupole and Ion-Trap Mass Spectrometry of Cardiolipin Standard and Its Deuterium Analog

To simplify data interpretation, we adopt the rules recommended by IUPAC with modification for designation of CL. Briefly, the three glycerol moieties are

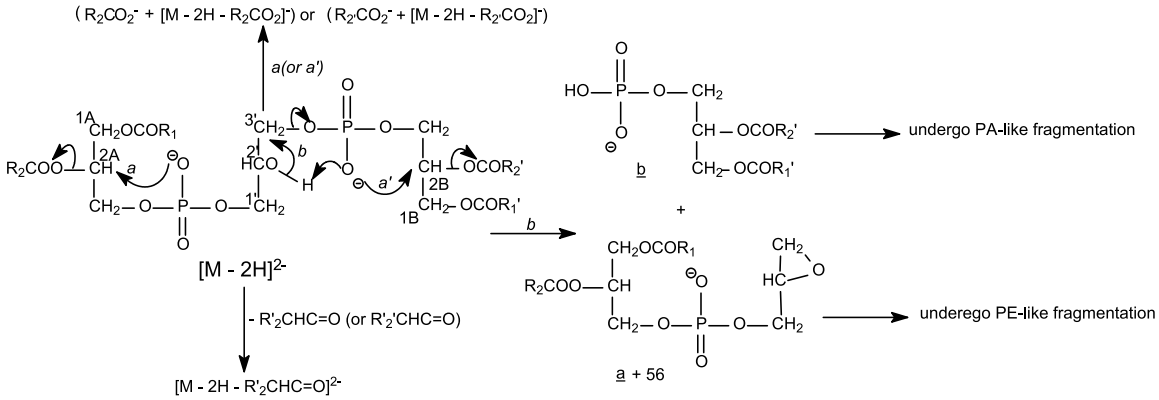

Scheme 1. The major fragmentation pathways proposed for the $[M - 2H]^{2-}$ ions of CL.

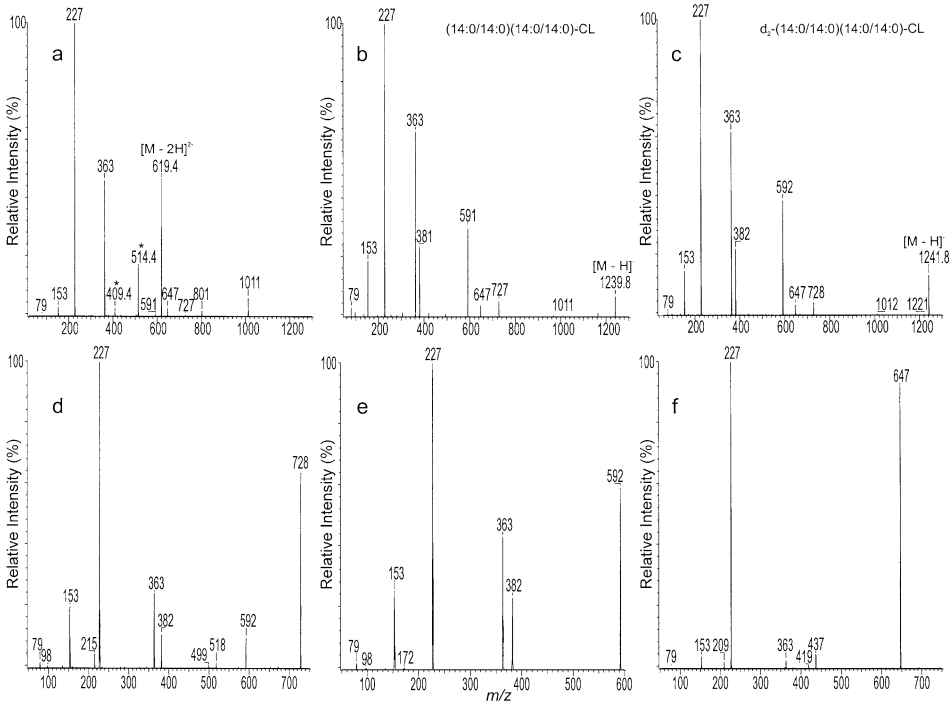

Figure 2. The tandem quadrupole product-ion spectra of (**a**) the $[M - 2H]^{2-}$ ion at *m/z* 619.6, (**b**) the $[M - H]^{-}$ ion at *m/z* 1239 of the (14:0/14:0)(14:0/14:0)-CL standard; (**c**) is the product-ion spectrum of the $[M - H]^{-}$ ion of d_2-(14:0/14:0)(14:0/14:0)-CL standard at *m/z* 1241, of which the exchangeable hydrogens have been substituted by deuterium atoms via H-D exchange. The mass shift(s) to *m/z* 1012 (from 1011), 728 (from 727), and 592 (from 591) observed in Figure 2c, along with the product-ion spectra of the *m/z* 728 (**d**), *m/z* 592 (**e**), and *m/z* 647 (**f**) ions generated by source CAD of the $[M - H]^{-}$ ion of d_2-(14:0/14:0)(14:0/14:0)-CL suggest the fragmentation pathways as proposed in Scheme **2**. The peaks labeled with a star symbol in all the figures denote doubly-charged fragment ions.

designated as A, B, and central glycerol (Scheme 1). The *stereospecific numberings* (*sn*) of the C1A and C2A carbons (Glycerol A) are designated as *sn*-1 and *sn*-2, respectively. The C1B and C2B carbons (Glycerol B) are designated as *sn*-1′ and *sn*-2′, respectively. The carbon number of the central glycerol is designated as C-1′, C-2′ and C-3′ with the C-1′ attached to the phosphatidic moiety with Glycerol A. Abbreviation of cardiolipin, such as (16:0/16:1)(18:0/18:1)-CL signifies that the 16:0-, 16:1-, 18:0-, and 18:1-fatty acyl substituents attach to C1A, C2A, C1B, and C2B, respectively.

The synthetic (14:0/14:0)(14:0/14:0)-CL standard contains four identical 14:0-acyl substituents residing at *sn*-1, *sn*-2 (Glycerol A), *sn*-1′ and at *sn*-2′ (Glycerol B). The compound gives an $[M - H]^{-}$ ion at *m/z* 1239 and an $[M - 2H]^{2-}$ ion at *m/z* 619.4. Selection and CAD of the $[M - 2H]^{2-}$ ions at *m/z* 619 (Figure 2a) at a collision energy of 22 eV yield the 14:0-carboxylate anion at *m/z* 227, reflecting the uniform fatty acyl moiety of the molecule. The product-ion spectrum also contains the *m/z* 514.4 ion, a doubly-charged fragment ion arising from loss of the 14:0-fatty acyl substituent as a ketene $(619.4 \times 2 - 210)/2$. However, ions corresponding to loss of the fatty acyl substituents as acids were not observed, consistent with the hypothesis that the $[M - 2H]^{2-}$ ion, which contains one less proton than does the $[M - H]^{-}$ ion, is a basic precursor ion and undergoes more facile ketene than acid loss [22]. The $R_xCO_2^{-}$ ion at *m/z* 227 mainly arises from nucleophilic attack of the anionic phosphate charge site onto C(2A) or C(2B) of the glycerol (Scheme 1). This fragmentation process also gives rise to *m/z* 1011 ($619 \times 2 - 227$).

In contrast, the $[M - H]^{-}$ ion at *m/z* 1239 yields the *m/z* 1011 (1239 − 228) ion by elimination of a tetradecanoic acid (Figure 2b) (in the IT MS^2-spectrum as shown in Figure 3b, this ion is more prominent). The spectrum also contains ions at *m/z* 591 (*a* and *b* ion), *m/z* 647 [(*b* + 56) and (*a* + 56)], and *m/z* 727 [(*a* + 136) and (*b* + 136)] (Scheme 2). The formation of these ions involves the participation of the exchangeable hydrogens. This is supported by the product-ion spectrum of d_2-(14:0/14:0)(14:0/14:0)-CL at *m/z* 1241 (Figure 2c), of which the exchangeable hydrogens at the central glycerol and at phosphate have been substituted by deuterium atoms via H—D exchange. The spectrum contains the analogous ions at *m/z* 592 and 728 with a mass shift of 1 Da, and at *m/z* 647 with no mass shift. This is consistent with the proposed mechanism as shown in Scheme **2** [the hydrogen atoms that were exchanged by deuterium atoms are denoted as "(D)"]. The *m/z* 591 is structurally equivalent to a deprotonated dimyristoyl phosphatidic (14:0/14:0-PA) anion, which arises from *m/z* 727 by neutral loss a tricylic glycerophosphate ester moiety of 136 (Scheme **2a**) [23–25]. This fragmentation

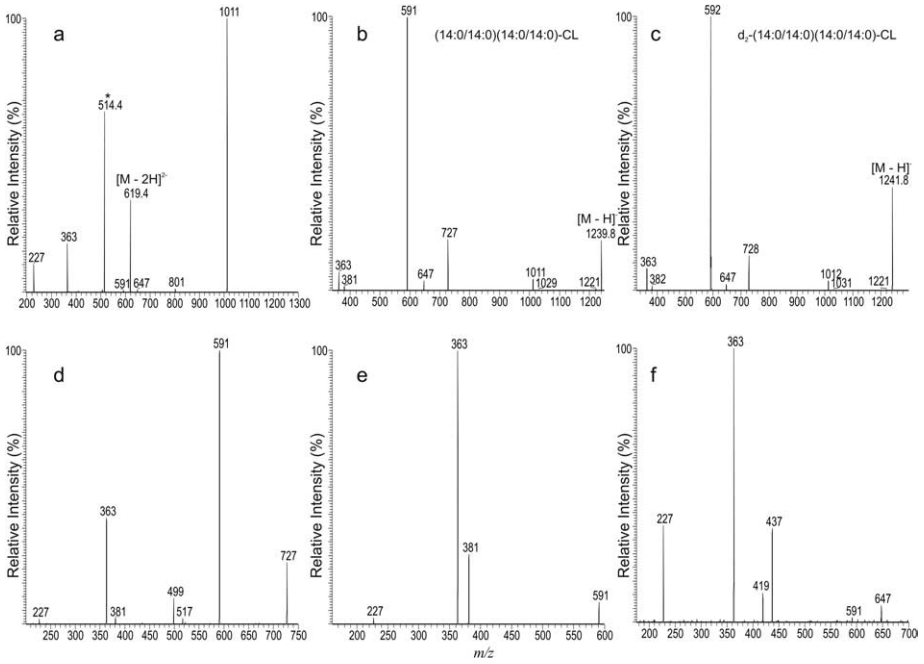

Figure 3. The ion-trap MS^2-spectra of (**a**) the $[M - 2H]^{2-}$ ion at *m/z* 619.4, (**b**) the $[M - H]^-$ ion at *m/z* 1239 of the (14:0/14:0)(14:0/14:0)-CL standard; (**c**) is the MS^2-spectrum of the $[M - H]^-$ ion of d_2-(14:0/14:0)(14:0/14:0)-CL (*m/z* 1241)prepared by H-D exchange. The MS^3-spectra of *m/z* 727 (1239 →727) (**d**), *m/z* 591 (1239 → 591) **e**), and *m/z* 647 (1239 → 647) (**f**) support the mechanisms depicted in Scheme **2**.

pathway is supported by the source-CAD product-ion spectrum of *m/z* 727 (not shown) arising from the $[M - H]^-$ ion of (14:0/14:0)(14:0/14:0)-CL at *m/z* 1239, and of the *m/z* 728 ion (Figure 2d) arising from the $[M - H]^-$ ion of d_2-(14:0/14:0)(14:0/14:0)-CL at *m/z* 1241. The spectrum is similar to the source-CAD product-ion spectrum of *m/z* 592 (Figure 2e) arising from *m/z* 1241, confirming the fragmentation process. The proposed structure of the *m/z* 647 ion [(*b* + 56) ion] resulting from the fragmentation process (Scheme **2b**) is also consistent with the hypothesis that the *m/z* 647 is a basic ion, which undergoes fragmentation processes similar to those observed for phosphatidylethanolamine (PE) and gives rise to a higher abundance of the *m/z* 437 ion (647 − 210) than of the *m/z* 419 ion (647 − 228) upon CAD (Figure 2f), due to the preferential loss of the 14:0 fatty acyl as a ketene than as an acid [26].

The ion-trap MS^2-spectra of the $[M - 2H]^{2-}$ ion (Figure 3a) and of the $[M - H]^-$ ion (Figure 3b) arising from (14:0/14:0)(14:0/14:0)-CL, and of the $[M - H]^-$ ion arising from d_2-(14:0/14:0)(14:0/14:0)-CL (Figure 3c) contain ions similar to those obtained with TSQ instrument. The IT MS^3-spectra of *m/z* 727 (1239 → 727) (Figure 3d), *m/z* 591 (1239 → 591) (Figure 3e), and *m/z* 647 (1239 → 647) (Figure 3f) also contain ions similar to those acquired by TSQ and further support the proposed mechanism. However, carboxylate anions at *m/z* 227 are not observed in Figures 3b and c because of low-mass cut-off nature of ITMS. The *m/z* 227 ion is of low-abundance in Figure 3b, consistent with the notion that the carboxylate anions observed in the product-ion spectra obtained by TSQ arise mainly from consecutive fragmentation processes [22, 23, 26].

Structural Characterization of Cardiolipins with Symmetric Acyl Moieties by CAD Product-Ion Spectra of the $[M - H]^-$ and $[M - 2H]^{2-}$ Ions

The carboxylate anion reflecting the fatty acyl substituent at *sn*-1 (or *sn*-1′) is more abundant than the corresponding ion reflecting that at *sn*-2 (or *sn*-2′) in the product-ion spectra of the $[M - H]^-$ ions, while the abundances of these two carboxylate ions are reversed in the product-ion spectra of the $[M - 2H]^{2-}$ ions. As shown in Figure 4, the $R_2CO_2^-$ (or $R_{2'}CO_2^-$) ion at *m/z* 253 is more abundant than the $R_1CO_2^-$ (or $R_{1'}CO_2^-$) ion at *m/z* 255 in the product-ion spectrum of the $[M - 2H]^{2-}$ ion of (16:0/16:1)(16:0/16:1)-CL at *m/z* 673.6 (Panel a) but the *m/z* 255 ion is more abundant than the *m/z* 253 ion in the product-ion spectrum of the $[M - H]^-$ ion at *m/z* 1347 (Panel b), obtained with a TSQ instrument. This reversal in the abundances of the carboxylate anions observed for precursors of cardiolipin with different charge states is similar to that reported for phosphatidylinositol bisphosphate [22] and provides complementary information to confirm the position of fatty acyl substituents on the glycerol backbone.

Both the 1′- and 3′-phosphate anionic sites of the $[M - 2H]^{2-}$ precursors render nucleophilic attack on the carbons of the glycerol backbone to which the fatty acyl

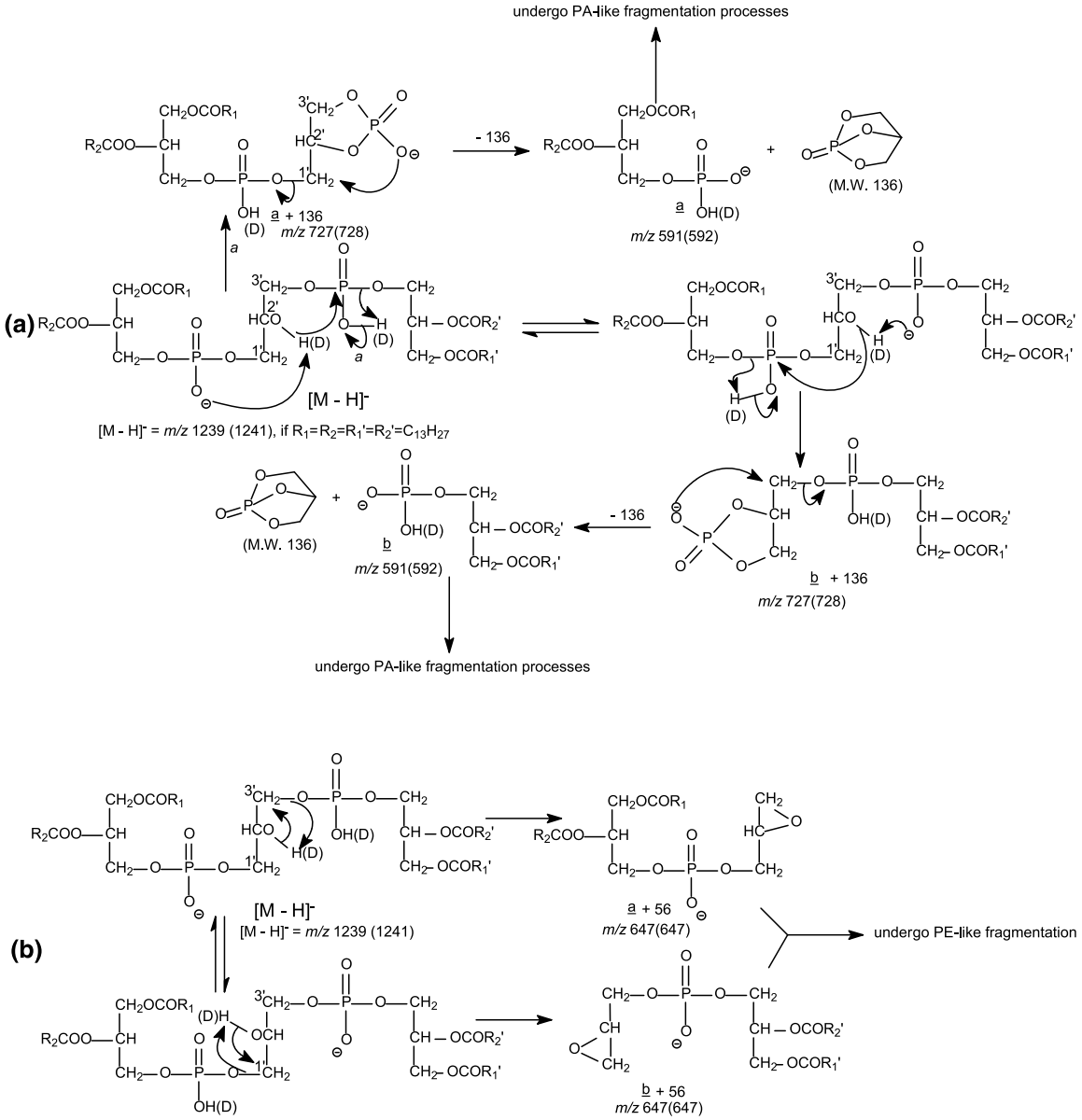

Scheme 2. The major fragmentation pathways proposed for formation (**a**) of the *a* (or *b*), a + 136 (or *b* + 136) ions and (**b**) of the *a* + 56 (or *b* + 56) ions for the $[M - H]^-$ ion of CL. The exchangeable hydrogens are denoted as "(D)". The *m/z* values expected for fragment ions of (14:0/14:0)(14:0/14:0)-CL and d_2-(14:0/14:0)(14:0/14:0)-CL (in parentheses) are shown.

substituents attached. The 1′-phosphate site attacks on the C(2A) and results in ions of *m/z* 1093 (673 × 2 − 253) and *m/z* 253 (16:1-carboxylate anion), simultaneously; while the attack on C(1A) resulting in ions of *m/z* 1091 (673 × 2 − 255) and 255 (16:0-carboxylate anion). The nucleophilic attack of the 3′-phosphate anionic site on C(2B) and C(1B) gives rise to the similar ions (Scheme **1**). The *m/z* 1093 ion is more abundant than the *m/z* 1091 ion and the *m/z* 253 ion is also more abundant than the *m/z* 255 ion in the spectrum. This is consistent with the notion that the mechanisms underlying the fragmentation processes for the gas-phase ions of $[M - 2H]^{2-}$ are similar to those observed for the $[M - H]^-$ ions of PE, and results in a greater abundance of $R_2CO_2^-$ (or $R_{2'}CO_2^-$) than of $R_1CO_2^-$ (or $R_{1'}CO_2^-$). This is attributable to the fact that the fragmentation processes leading to the ion formation are sterically more favorable at *sn*-2 than at *sn*-1 [22–26]. The loss of the fatty acyl substituent at *sn*-2 or at *sn*-2′ as fatty acyl ketene leads to a doubly-charged fragment ion at *m/z* 555.5 (673.5 × 2 – 236)/2, which is more abundant than the *m/z* 554.5 (2 × 673.5 – 238)/2 ion, a doubly-charged fragment ion arising from the similar loss at *sn*-1 or at *sn*-1′. The charge states of the above two ions are confirmed by the tandem mass spectrum of the same ions obtained with a Q-TOF instrument (data not shown), which provides sufficient resolution to show the charge state. This preferential formation of the ions reflecting the ketene

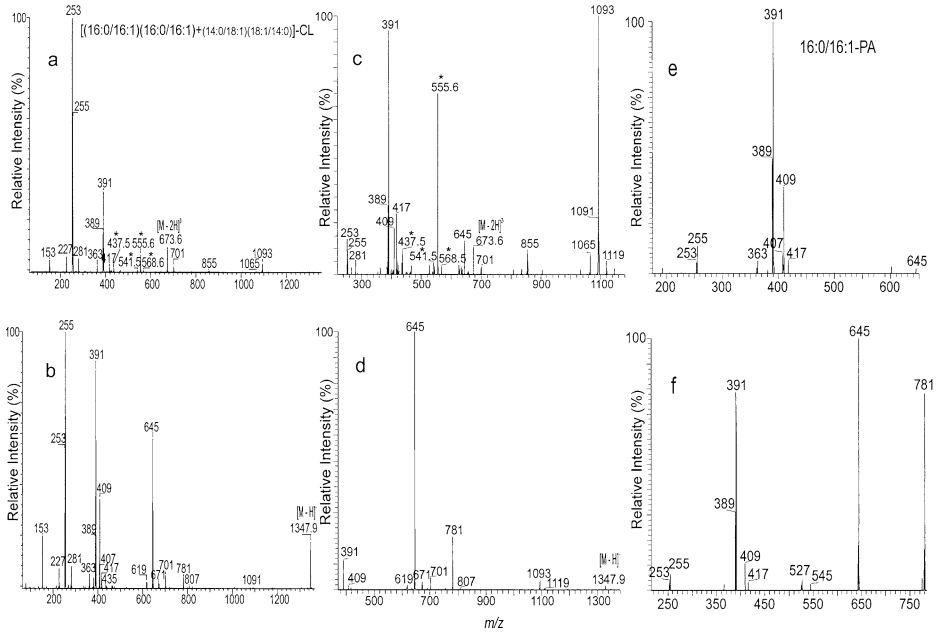

Figure 4. The tandem quadrupole product-ion spectra of the $[M - 2H]^{2-}$ ion at *m/z* 673.6 (**a**), and of the $[M - H]^{-}$ ion at *m/z* 1347 (**b**); (**c** and (**d**) are the IT MS^2-spectra of the $[M - 2H]^{2-}$ ion at *m/z* 673.6 (**c**), and of the $[M - H]^{-}$ ion at *m/z* 1347 (**d**) from bacterium *Salmonella typhimurium*; (**e** and **f**) are the IT MS^3-spectra of *m/z* 645 (1347 → 645) (**e**), and *m/z* 781 (1347 → 781) (**f**). The structural assignments of the major (16:0/16:1)(16:0/16:1)-CL species along with a minor (14:0/18:1)(18:1/14:0)-CL isomer are supported by the various tandem mass spectra shown above.

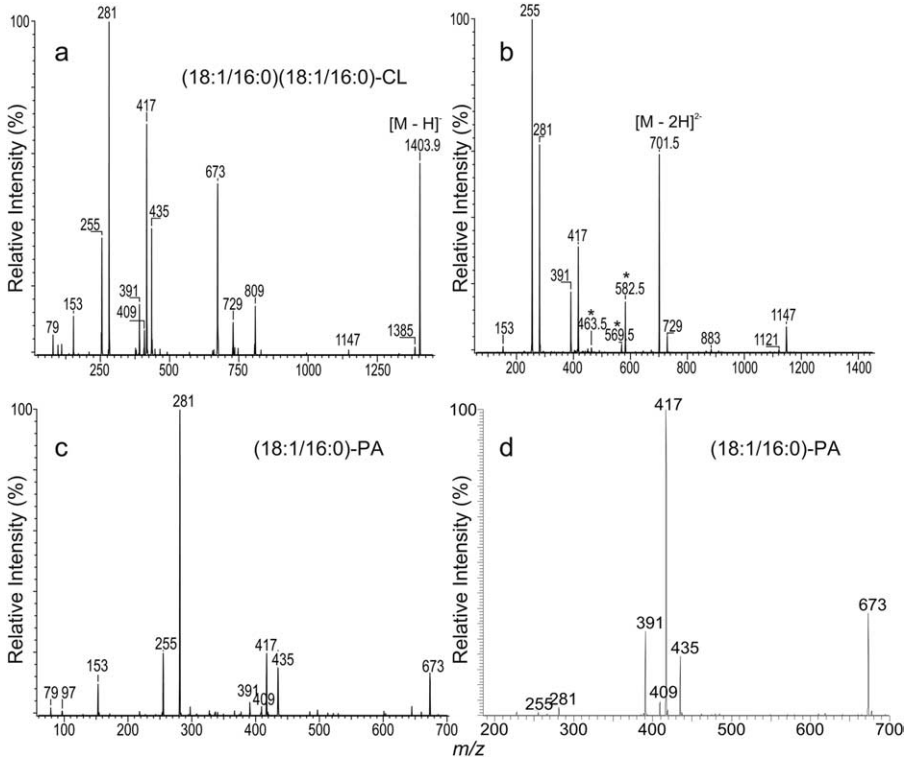

Figure 5. The tandem quadrupole mass spectra of (**a**) the $[M - H]^{-}$ ion at *m/z* 1403 and (**b**) the $[M - 2H]^{2-}$ ion at *m/z* 701.5 from cardiolipin mixture isolated from *Mycobacterium bovis*. Both the product-ion spectrum of *m/z* 673 (**c**) from source CAD and the IT MS^3-spectrum of *m/z* 673 (1403 → 673) (**d**) identify the symmetric 18:1/16:0-PA moiety of the molecule and lead to identify the (18:1/16:0)(18:1/16:0)-CL structure.

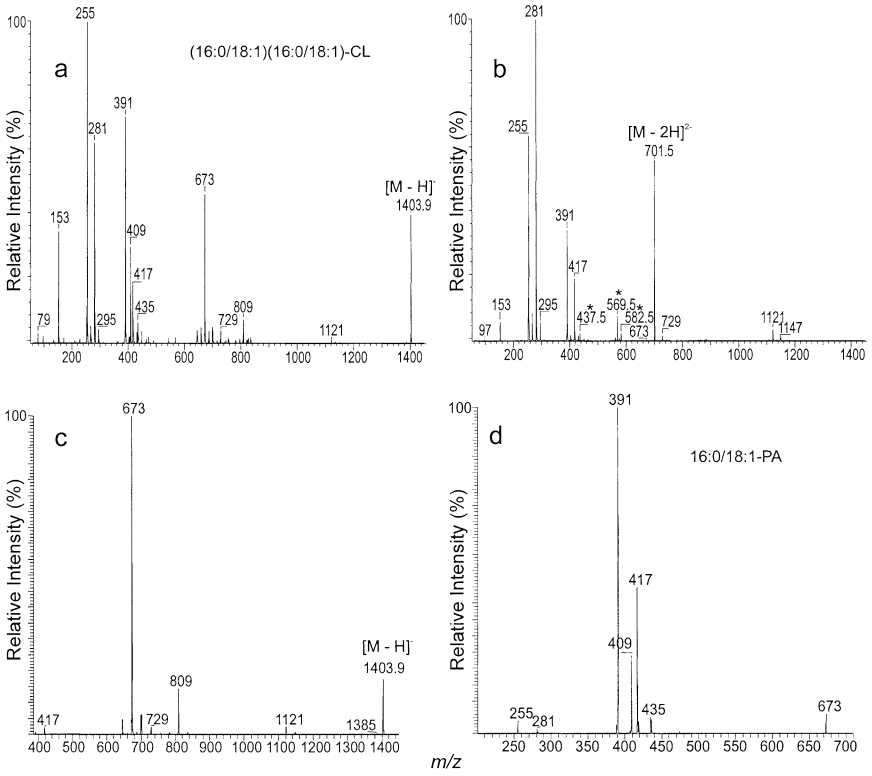

Figure 6. The tandem quadrupole mass spectra of (**a**) the $[M - H]^-$ ion at *m/z* 1403 and (**b**) the $[M - 2H]^{2-}$ ion at *m/z* 701.5, and (**c**) the IT MS^2-spectrum of the $[M - H]^-$ ion at *m/z* 1403 from the cardiolipin mixture isolated from bacterium *Salmonella typhimurium*. The IT MS^3-spectrum of the *m/z* 673 (1403 → 673) ion (**d**) is identical to that arising from 16:0/18:1-PA. The assignment of the major isomeric structure of (16:0/18:1)(16:0/18:1)-CL is consistent with that described in Figure 5.

loss at *sn*-2 (or *sn*-2′) over that at *sn*-1 (or *sn*-1′) is also consistent with the concept as described earlier and permits structural determination of complex CL molecules, including configuration isomer and positional isomers as described later. The IT MS^2-spectrum of the $[M - 2H]^{2-}$ ions at *m/z* 673.5 (Panel c) contains ions similar to those observed in Figure 4a, but ions at *m/z* 1093 and 555.6 are among the most prominent and the carboxylate anions at *m/z* 253 and 255 are of low abundance. This is in accord with the results observed for (14:0/14:0)(14:0/14:0)-CL (Figure 2a).

The product-ion spectra of the $[M - H]^-$ ion at *m/z* 1347 obtained with a TSQ instrument (Panel b) and with an IT instrument (Panel d) contain ions at *m/z* 645 (*a* and *b*), 701 [(a + 56) and (*b* + 56)], and 781 [(a + 136) and (b + 136)], resulting from the fragmentation processes involving the exchangeable hydrogens as described earlier (Scheme **2**), and these ions are more prominent in the IT MS^2-spectrum (Figure 4d). The MS^3-spectrum of the *m/z* 645 ion (1347 → 645) (Figure 4e) is identical to that arising from the $[M - H]^-$ ion of 16:0/16:1-PA, which contains major fragment ions at *m/z* 391 and 389 arising from loss of the palmitoleic acid (16:1) at *sn*-2 and loss of the palmitic acid (16:0) at *sn*-1, respectively [23]. This confirms assignment of the (16:0/16:1)(16:0/16:1)-CL structure. The MS^3-spectrum of the *m/z* 781 ion (Figure 4f) contains a major ion at *m/z* 645 and fragment ions similar to those observed in the MS^3-spectrum of *m/z* 645, indicating that *m/z* 781 is precursor ion of *m/z* 645 and undergoes further dissociation to *m/z* 645 (781 − 136) via neutral loss of a stable tricyclic glycerophosphate ester (136 Da), similar to that described earlier.

In Figures 4a and b, the spectra also contain a minor set of the carboxylate anions at *m/z* 281 (18:1) and 227 (14:0), indicating the presence of an isobaric structure consisting of 18:1- and 14:0-fatty acyl substituents. The results are in accord with the observation of *m/z* 1119 (673 × 2 − 227) and *m/z* 1065 (673 × 2 − 281) ions in the Figure 4c, probably arising from a (14:0/18:1)(18:1/14:0)-CL [or a (18:1/14:0)(14:0/18:1)-CL] isomer. This speculation is based on the fact that the two ions are nearly equal abundance. The ions at *m/z* 281 and 227 are also equally abundant in the product-ion spectra of both the $[M - H]^-$ ion at *m/z* 1347 (Figure 4a) and of the $[M - 2H]^{2-}$ ion at *m/z* 673.6 (Figure 4b). The structure of this isomer is further recognized by the observation of the ions at *m/z* 417 (645 − 228) and *m/z* 363 (645 − 282), arising from losses of 14:0- and 18:1-fatty acids, respectively, in the MS^3-spectrum of the *m/z* 645 ion (1345 → 645) (Figure 4e). The abundances of the ions at *m/z* 417 and at *363* are nearly identical, indicating the presence of both a 18:1/14:0-PA and a 14:0/18:1-PA isomer.

The observation in the differences in abundances of the

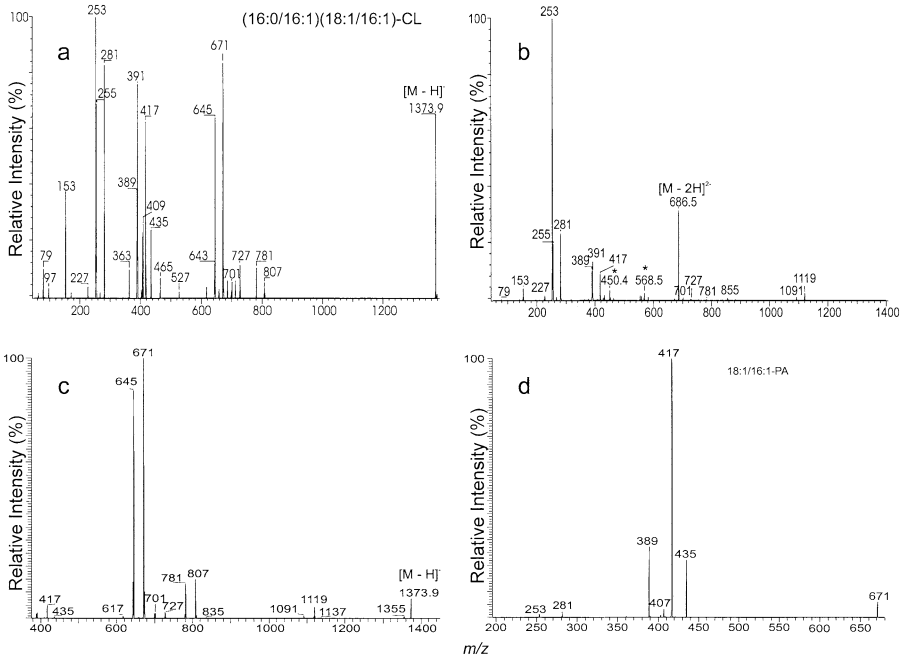

Figure 7. The tandem quadrupole mass spectra of the $[M - H]^-$ ion at *m/z* 1373 (**a**) and of the $[M - 2H]^{2-}$ ion at *m/z* 686.5 (**b**) from cardiolipin mixture isolated from bacterium *Salmonella typhimurium*. The IT MS^2-spectrum of the $[M - H]^-$ ion at *m/z* 1373 is shown in (**c**), and the MS^3-spectrum of the *m/z* 671 ion (1373 → 671) is shown in (**d**). The information from these spectra combined identifies the major (16:0/16:1)(18:1/16:1)-CL structure.

carboxylate anions leading to the structural characterization of CL is further demonstrated by the product-ion spectra of the $[M-H]^-$ ion at *m/z* 1403 (Figure 5a) and the $[M-2H]^{2-}$ ion at *m/z* 701.6 (Figure 5b), observed for the lipid extract from *Mycobacterium bovis* BCG. The *m/z* 281 ion (18:1) is more abundant than the *m/z* 255 ion (16:0) in the product-ion spectrum of *m/z* 1403 (Figure 5a), a singly-charged ion. However, the abundances of the two ions are reversed in the product-ion spectrum of the $[M - 2H]^{2-}$ ion at *m/z* 701.6 (Figure 5b). The results suggest that the 18:1- and 16:0-fatty acyl substituents probably reside at *sn*-1 (or *sn*-1′) and *sn*-2 (or *sn*-2′), respectively. This assignment is further supported by observation of a greater abundance of the *m/z* 1147 (701 × 2 – 255) ion than the *m/z* 1121 (701 × 2 − 281) ion and a greater abundance of the *m/z* 582.6 ion (701.6 × 2 – 238)/2 than the *m/z* 569.6 (701.6 × 2 – 264)/2 ion in the product-ion spectrum of the $[M - 2H]^{2-}$ ion at *m/z* 701.6 (Figure 5b). In Figure 5a, the spectrum contains the prominent ion set of *m/z* 673 (*a* & *b*), 729 [(*a* + 56) and (*b* + 56)] and 809 [(*a* + 136) and (*b* + 136)]. The identities and positions of the fatty acyl substituents are recognized by the source CAD product-ion spectrum of *m/z* 673 (Figure 5c), which is identical to that of 18:1/16:0-PA obtained with a triple quadrupole instrument. The IT MS^2-spectrum of the *m/z* 673 ion (1403 → 673) (Figure 5d) is also identical to the MS^2-spectrum of 18:1/16:0-PA, which is featured by that the *m/z* 417 ion (673 − 256) arising from loss of 16:0-acid is more abundant than *m/z* 391 (673 − 282, arising from loss of 18:1-acid; and that the *m/z* 435 ion (673 − 238) arising from loss of 16:0-ketene is more abundant than *m/z* 409 (673 − 264), arising from loss of 18:1-ketene. The MS^2-spectra in combination with the MS^3-spectra described above suggest that the compound represents a (18:1/16:0)(18:1/16:0)-CL structure.

In the lipid extract from bacterium *Salmonella typhimurium*, the *m/z* 255 ion is more abundant than the *m/z* 281 ion in the product-ion spectrum of the $[M - H]^-$ ion at *m/z* 1403 (Figure 6a), while the abundances of the two ions are reversed in the product-ion spectrum of the $[M - 2H]^{2-}$ ion at *m/z* 701.6 (Figure 6b). These results are opposite to those observed for (18:1/16:0)(18:1/16:0)-CL as shown in Figure 5a and b. The MS^2-spectra of the $[M - H]^-$ ion at *m/z* 1403 obtained with a TSQ instrument (Figure 6a) and with IT instrument (Figure 6c) also contain the ion set of *m/z* 673, 729, and 809 similar to those observed in Figure 5a, indicating that the compound may represent a positional isomer. The identities and positions of the fatty acyl substituents are further recognized by the MS^3-spectrum of *m/z* 673 (1403 → 673) (Figure 6d), which is identical to that arising from 16:0/18:1-PA and clearly reveals the structure of (16:0/18:1)(16:0/18:1)-CL.

Structural Characterization of Cardiolipins Containing Different Diacylglycerol Moieties by CAD Product-Ion Spectra of the $[M - H]^-$ and $[M - 2H]^{2-}$ Ions

The characterization of cardiolipin consisting of two various diacylglycerol moieties is illustrated by the

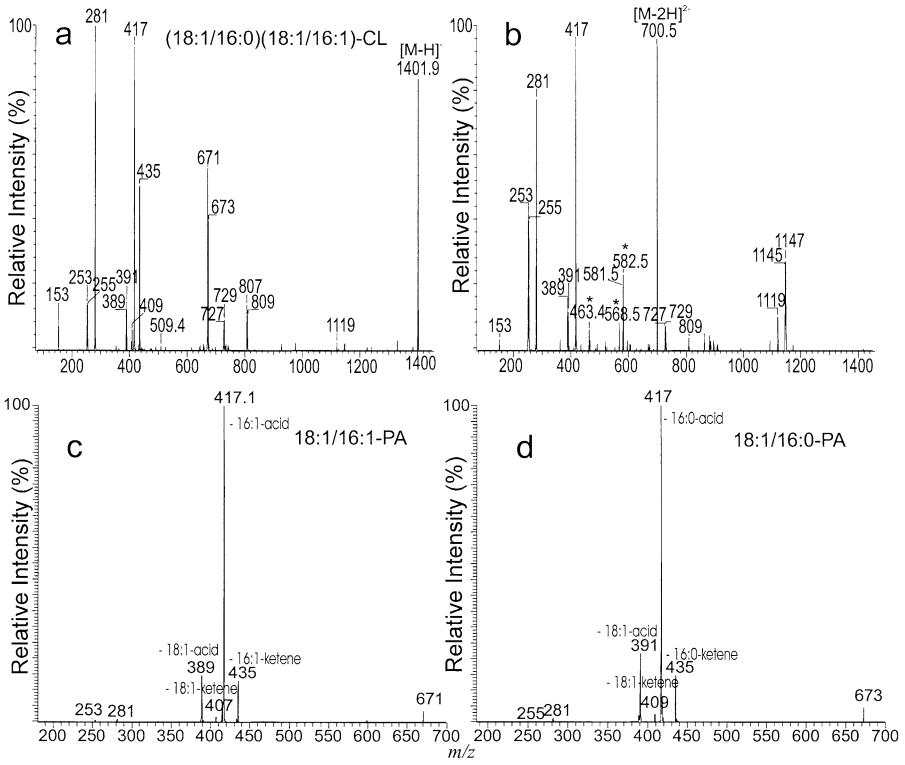

Figure 8. The tandem quadrupole mass spectra of the $[M - H]^-$ ion at *m/z* 1401 (**a**) and the $[M - 2H]^{2-}$ ion at *m/z* 700.5 (**b**) from cardiolipin mixture isolated from *Mycobacterium bovis*. The IT MS^3-spectra of (**c**) *m/z* 671 (1401 → 671), and (**d**) *m/z* 673 (1401 → 673) confirm the 18:1/16:0-PA and 18:1/16:1-PA structures, respectively. The assignment of the (18:1/16:0)(18:1/16:1)-CL structure is also determined by the fact that the *m/z* 671 ion is more abundant than the *m/z* 673 ion.

product-ion spectra of the *m/z* 1373 ion obtained with a TSQ instrument (Figure 7a) and with an ITMS (Figure 7b). Both spectra contain the ion sets of *m/z* 671 (*a* ion), 727 (*a* + 56), 807 (*a* + 136) and of *m/z* 645 (*b*), 701 (*b* + 56), 781 (*b* + 136). The MS^3-spectrum of the *m/z* 645 ion (1373 → 645) (data not shown) in the latter set is identical to that observed in Figure 4e, suggesting a 16:0/16:1-PA configuration. The MS^3-spectrum of *m/z* 671 (1373 → 671) (Figure 7d) of the former set is dominated by the *m/z* 417 ion, arising from a 16:1-acid loss at *sn*-2′, and the less prominent ion at *m/z* 389 arising from loss of the 18:1-acid at *sn*-1′, exhibiting a 18:1/16:1-PA structure. These results indicate that the *m/z* 1373 ion probably represents a (18:1/16:1)(16:0/16:1)-CL. The *m/z* 671 (*a*) is more abundant than *m/z* 645 (*b* ion) in the MS^2-spectrum of the $[M - H]^-$ ion at *m/z* 1373, consistent with the notion that cardiolipin contains two chemically distinct phosphatidyl moieties [2, 27, 28]. The observation of a greater abundance of the *m/z* 671 ion than the *m/z* 645 ion may indicate that the 18:1/16:1-glycero moiety is attached to the 1′ position of the central glycerol. This speculation is based on the fact that the H^+ on the phosphate attached to *sn*-3 (pK_1 = 2.8) is more acidic than that at *sn*-3′ (pK_2 > 7.5) [28] and the anionic charge site may more favorably reside at *sn*-3′ phosphate and initiates the cleavage of P—O bond via a charge-driven process with the participation of the exchangeable hydrogen as shown in Scheme **2a** (route *a*). This fragmentation process also results in expulsion of a diacylglycerol and gives rise to an *m/z* 807 (*a* + 136) ion, which dissociates to *m/z* 671 (*a*) by loss of a tricyclic glycerophosaphate ester of 136 Da as described earlier.

The carboxylate anions were observed at *m/z* 281 (18:1), 255 (16:0), and 253 (16:1), and the *m/z* 253 ion is 5-fold the abundance of *m/z* 255 and of *m/z* 281 in the product-ion spectrum of the $[M - 2H]^{2-}$ ion at *m/z* 686.5 (Figure 7b). This is consistent with the notion that the $[M - 2H]^{2-}$ ion at *m/z* 686.5 is a basic ion and undergoes fragmentation processes similar to those observed for PE [26], resulting in more favorable formation of the $R_2CO_2^-$ (or $R_{2'}CO_2^-$) anions than of the $R_1CO_2^-$ (or $R_{1'}CO_2^-$) ions. The results are also consistent with the fact that the molecule consists of two palmiteoyl fatty acyl substituents, respectively residing at *sn*-2 and *sn*-2′, and one palmitoyl residing at *sn*-1 and one oleoyl residing *sn*-1′. In contrast, differences in the abundances among the *m/z* 253, 255, and 281 ions are not substantial in the product-ion spectrum of the $[M - H]^-$ ion at *m/z* 1373 (Figure 7a), which undergoes fragmenatations similar to those observed for PA (23). The fragmentation processes occurred to the $[M - 2H]^{2-}$ ion at *m/z* 686.5 also result in the preferential loss of the fatty acyl substituents at *sn*-2 (or *sn*-2′) as ketene and leads to

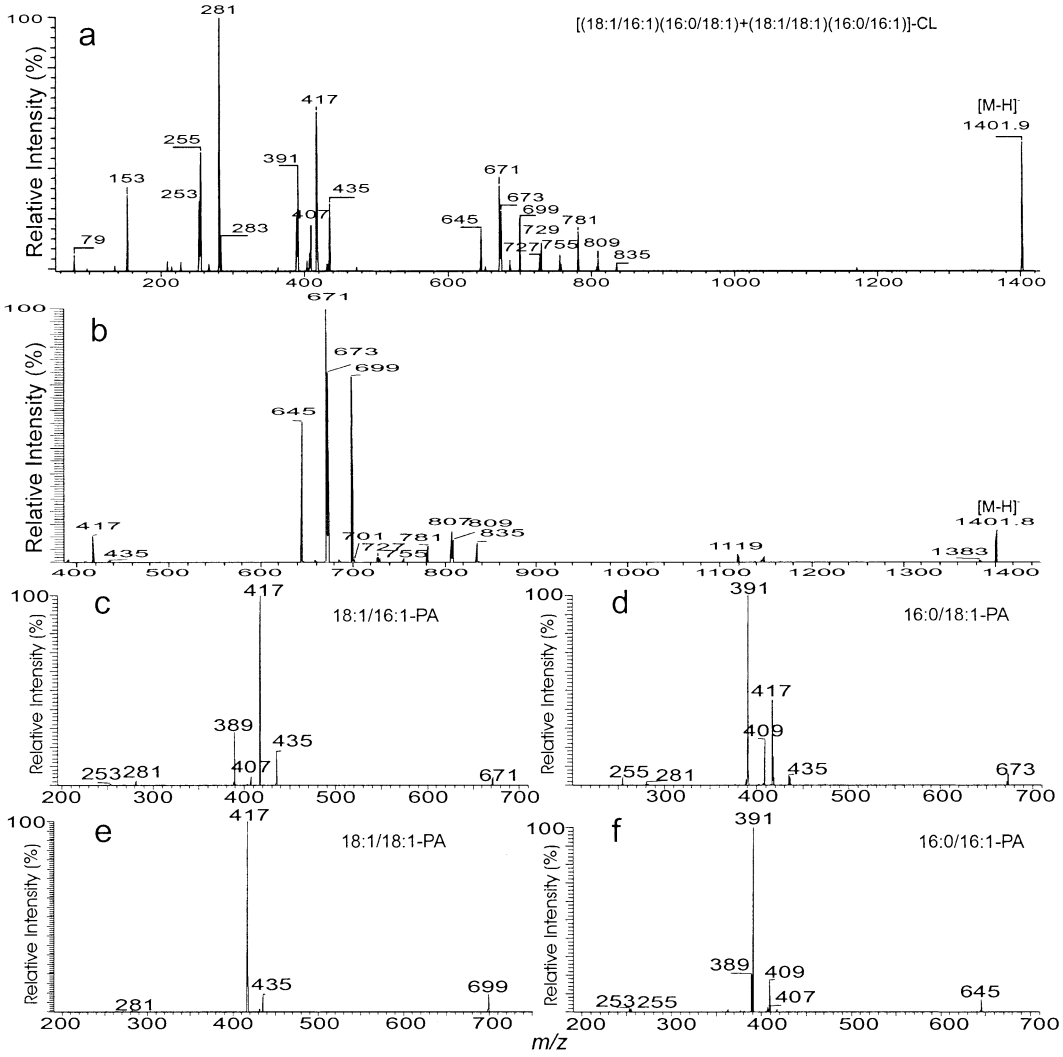

Figure 9. The tandem mass spectra of the $[M - H]^-$ ions of *m/z* 1401 obtained with (**a**) a TSQ instrument, (**b**) with an ITMS. The IT MS^3-spectra of *m/z* 671 (1401 → 671) (**c**), *m/z* 673 (1401 → 673) (**d**), *m/z* 699 (1401 → 699) (**e**), and *m/z* 645 (1401 → 645) (**f**) provide information for locating the fatty acyl substituents. The structural information from the above spectra combined suggests that the species consists of a major (18:1/16:1)(16:0/18:1)-CL along with a (18:1/18:1)(16:0/16:1)-CL isomer.

formation of a doubly-charged fragment ion at *m/z* 568.5 (686.5 × 2 – 236)/2, arising from loss of the 16:1-fatty acyl ketene at *sn*-2 (or *sn*-2′). The preferential attack of the anionic charge site on C(2A) [or C(2B)] of the glycerol also results in more favorable formation of *m/z* 1119 (686 × 2 − 253) than of *m/z* 1117 (686 × 2 − 255) (not seen) or of *m/z* 1091 (686 × 2 − 281) that arises from the similar attack on C(1A) [or C(1B)], and provide information to confirm the position of fatty acyl substituents on the glycerol backbone.

The tandem quadrupole mass spectra of the $[M - H]^-$ ion at *m/z* 1401 (Figure 8a) and of the $[M - 2H]^{2-}$ ion at *m/z* 700.5 (Figure 8b) arising from the lipid extract of *Mycobacterium bovis* BCG contain carboxylate anions at *m/z* 281 (18:1), 253 (16:1) and 255 (16:0). The structural determination is established by the observation of the ion sets of *m/z* 671 (*a*), 727 (*a* + 56), 807 (*a* + 136) and of *m/z* 673 (*b*), 729 (*b* + 56), 809 (*b* + 136). The two ion sets reflect a 18:1/16:1- and a 18:1/16:0-phosphatidyl moiety, respectively, as evidenced by the source-CAD tandem mass spectra of *m/z* 671 and 673 (not shown), and further confirmed by the IT MS^3-spectra of *m/z* 673 (1401 → 673) (Figure 8c) and 671 (1401 → 671) (Figure 8d). Since the former ion set is more abundant than the latter, a (18:1/16:1)(18:1/16:0)-CL structure can be easily assigned. In the product-ion spectrum of the $[M - 2H]^{2-}$ ion at *m/z* 700.5 (Figure 8b), the *m/z* 1147 (700 × 2 − 253) and 1145 (700 × 2 − 255) ions, reflecting the $R_2CO_2^-$ and $R_2'CO_2^-$ losses, respectively, are more abundant than *m/z* 1119 (700 × 2 − 281), reflecting the $R_1CO_2^-$ (or $R_1'CO_2^-$) loss. The doubly-charged ions at *m/z* 582.5 (700.5 × 2 − 236)/2 and at *m/z* 581.5 (700.5 × 2 − 238)/2 arising from the respective 16:1- and 16:0-acyl losses as ketenes are also more abundant than

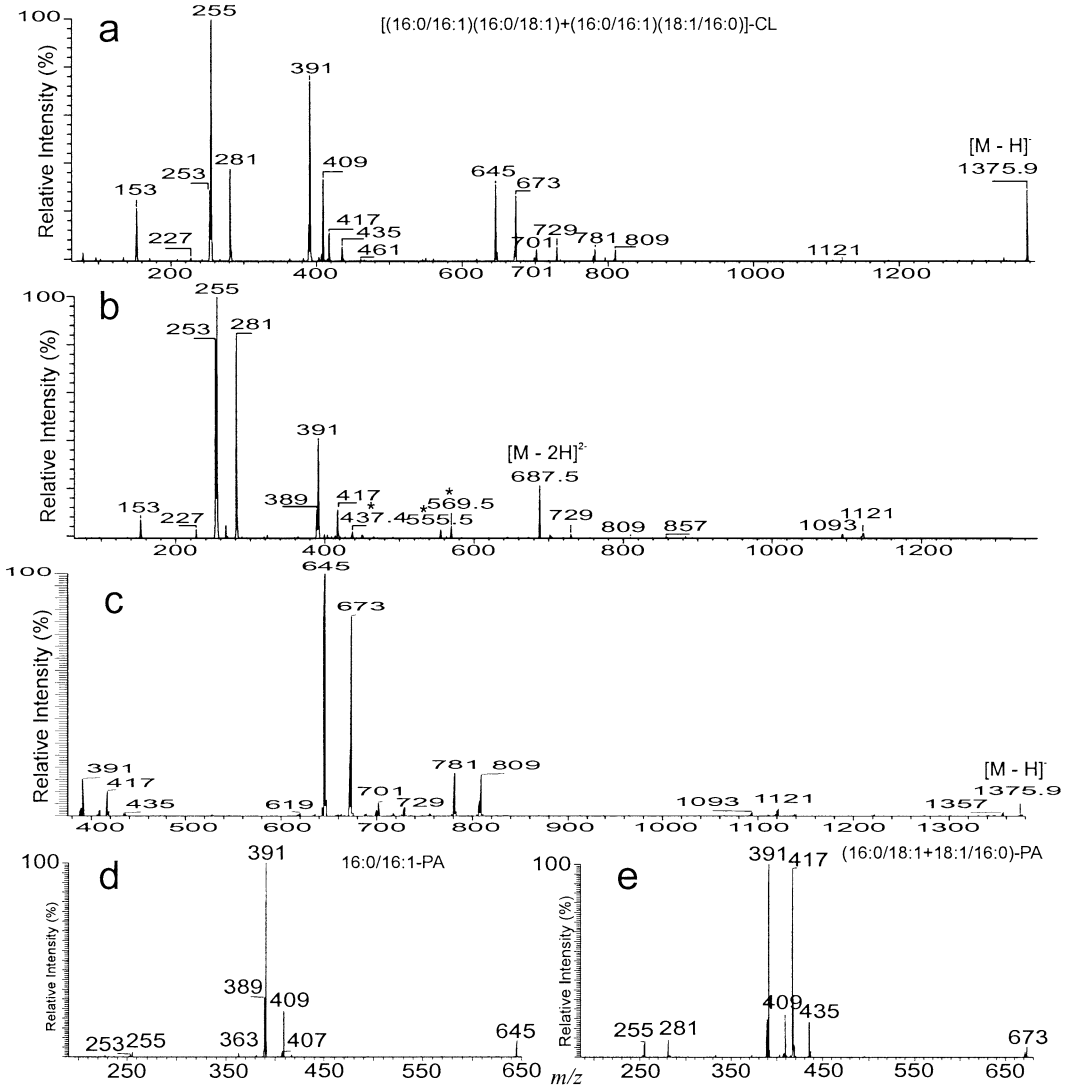

Figure 10. The product-ion spectra of (**a**) the $[M - H]^-$ ion at *m/z* 1375 and (**b**) the $[M - 2H]^{2-}$ ion at *m/z* 687.5 obtained with a TSQ instrument. The IT MS^2-spectrum of the $[M - H]^-$ ions at *m/z* 1375 is shown in (**c**), which contains ions similar to those observed in (**a**) and (**b**), but carboxylate anions are absent because of low-mass cutoff. The IT MS^3-spectrum of *m/z* 645 (1375 → 645) (**d**) is typical of 16:0/16:1-PA, and the MS^3-spectrum of *m/z* 673 (1375 → 673) (**e**) is probably a mixed spectra consisting of both a 16:0/18:1- and an 18:1/16:0-PA. The combined information suggests that the molecules are isomers of (16:0/16:1)(16:0/18:1)-CL and (16:0/16:1)(18:1/16:0)-CL.

m/z 568.5 (700.5 × 2 − 264)/2, arising from loss of a 18:1-acyl moiety as a ketene. These results further confirm the assignment of the positions of the fatty acyl substituents of the molecule.

Structural Characterization of Cardiolipin Molecular Species with Multiple Isobaric Isomers

Structural characterization of cardiolipins of biological origin is often complicated by numerous homologs that consist of various isomers (Figure 1). For examples, the product-ion spectra of *m/z* 1401 ions obtained with a TSQ instrument (Figure 9a) and with an ITMS (Figure 9b) arising from the lipid extract of bacterium *Salmonella typhimurium* contain prominent ion set of *m/z* 671 (*a*), 727 (*a* + 56), and 807 (*a* + 136), along with the ion set of *m/z* 673 (*b*), 729 (*b* + 56), 809 (*b* + 136). The *m/z* 671 is more abundant than *m/z* 673, suggesting the presence of the (18:1/16:1)(16:0/18:1)-CL isomer. This structure is further confirmed by the MS^3-spectra of *m/z* 671 (1401 → 671, Figure 9c) and *m/z* 673 (1401 → 673, Figure 9d), which are equivalent to 18:1/16:1-PA and 16:0/18:1-PA, respectively. The tandem mass spectra (Figure 9a and b) also contain the ion set at *m/z* 699 (*a*), 755 (*a* + 56), and 835 (*a* + 136), along with its complementary ion set at *m/z* 645 (*b*), 701 (*b* + 56), and 781 (*b* + 136), suggesting the presence of a second isomer, probably representing a (18:1/18:1)(16:0/16:1)-CL. This speculation, again, is based on the findings that the *m/z* 699 ion is

more abundant than *m/z* 645, and further confirmed by the MS^3-spectrum of *m/z* 699 (1401 → 699, Figure 9e), which is equivalent to 18:1/18:1-PA and of *m/z* 645 (1401 → 645, Figure 9f) representing a 16:0/16:1-PA. Structural determination of complex CL containing multiple isomeric structures are further demonstrated by the product-ion spectra of the $[M - H]^-$ ion at *m/z* 1375 (Figure 10a) and the $[M - 2H]^{2-}$ ion at *m/z* 687.5 (Figure 10b) observed in the lipid extract from bacterium *Salmonella typhimurium*. The two spectra contain the carboxylate anions at *m/z* 281, 255, and 253, reflecting the 18:1, 16:0 and 16:1-fatty acyl substituents, respectively. The tandem mass spectra of the *m/z* 1375 ion obtained with an TSQ instrument (Figure 10a) and ITMS (Figure 10c) contain two ion sets observed at *m/z* 645 (*a*), 701 (*a* + 56) and 781 (*a* + 136), and at *m/z* 673 (*b*), 729 (*b* + 56) and 809 (*b* + 136). The $IT\text{-}MS^3$-spectra of *m/z* 645 (1375 → 645) (Figure 10d) clearly identify the 16:0/16:1-PA moiety, as supported by observation of the preferential loss of the 16:1- over the 16:0-fatty acyl moiety. However, ions at *m/z* 417 (673 − 256) and 391 (673 − 282), corresponding to losses of 16:0- and 18:1-fatty acids, respectively, are nearly equal abundance in the IT MS^3-spectrum of *m/z* 673 (1375 → 673) (Figure 10e), indicating that the *m/z* 673 ion probably represents isomers of 16:0/18:1-PA and 18:1/16:0-PA. This speculation is based on the MS^3-spectra of the *m/z* 673 ions observed in Figure 8f arising from 18:1/16:0-PA, and in Figure 9d arising from a 16:0/18:1-PA isomer. The speculation is also consistent with the fact that ions at *m/z* 255 and 281 are also nearly equally abundant (Figure 10e). The results suggest that the ion species mainly consist of both a (16:0/16:1)(18:1/16:0)-CL and a (16:0/16:1)(16:0/18:1)-CL isomer.

Conclusions

The above results demonstrate that structural characterization of cardiolipin can be achieved by multiple stage (MS^3) tandem mass spectrometry with ESI in negative-ion mode. The tandem quadrupole product-ion spectra or the MS^2-spectra from ITMS provide structural information regarding the identity of the fatty acyl substituents and the information for assignment of the diacylphosphatidyl moieties attached to 1′- or 3′ position of the central glycerol. The MS^3-spectra or source CAD product-ion spectra of the diacylphosphatidyl fragment anions provide the structural information to reveal the position of the fatty acyl substituents on the glycerol backbone. Product-ion spectra arising from the $[M - 2H]^-$ ions are also useful and provide complementary information to confirm the structure. However, standard cardiolipins with various fatty acyl substituents are required to confirm the assignment described above. The limited mass window for precursor ion selection in ITMS and TSQ instrument has also restricted its application in this study, because homologous ions differentiated by two daltons in biological extract are often inseparable from isotopic ions and therefore are subjected to collision dissociation simultaneously. In addition, assignment of doubly-charged fragment ions is also restricted by the limited resolving power of the quadrupole analyzers. More improvements in resolution and in selectivity of precursor ions are required for unambiguous structure characterization. Therefore, the implementation of analyses with high resolving power instrument with MS^n capability, such as FT-ICR, may have an impact in the structural determination of more complex lipids such as CL in future.

Acknowledgments

This research was supported by US Public Health Service grants P41-RR-00954, R37-DK-34388, P60-DK-20579, P01-HL-57278, P30-DK-56341 and a grant (996003) from the Juvenile Diabetes Foundation.

References

1. LeCocq, J.; Ballou, C. E. On the structure of cardiolipin. *Biochemistry* **1964,** *155*, 976–980.
2. Powell, G. L.; Jacobus, J. The nonequivalence of the phosphorus atoms in cardiolipin. *Biochemistry* **1974,** *13*, 4024–4026.
3. Pangborn, M. C. Isolation and purification of a serologically active phospholipid from beef heart. *J. Bio. Chem.* **1942,** *143*, 247–256.
4. White, D. A. The phospholipid composition of mammalian tissues. In *Form and function of phospholipids*; Ansell, G. B.; Hawthorne, J. N.; Dawson, R. M. C., Eds.; Elsevier Publishing: New York, NY, 1973; p 441.
5. Hatch, G. M. Cardiolipin: Biosynthesis, remodeling and trafficking in the heart and mammalian cells. *Int. J. Mol. Med.* **1998,** *1*, 33–41.
6. Hatch, G. M. Regulation of cardiolipin biosynthesis in the heart. *Mol. Cell Biochem.* **1996,** *159*, 139–148.
7. Ostrander, D. B.; Sparagna, G. C.; Amoscato, A. A.; McMillin, J. B.; Dowhan, W. Decreased cardiolipin synthesis corresponds with cytochrome *c* release in palmitate-induced cardiomyocyte apoptosis. *J. Biol. Chem.* **2001,** *276*, 38061–38067.
8. McMillin, J. B.; Dowhan, W. Cardiolipin and apoptosis. *Biochim. Biophys. Acta* **2002,** *1585*, 97–107.
9. Hoch, F. L. Cardiolipin and biomembrane function. *Biochim Biophys. Acta* **1992,** *1113*, 71–133.
10. Valianpour, F.; Wanders, R. J. A.; Barth, P. G.; Overmars, H.; van Gennip, A. H. Quantitative and compositional study of cardiolipin in platelets by electrospray ionization mass spectrometry: Application for the identification of Barth syndrome patients. *Clin. Chem.* **2002,** *48*, 1390–1397.
11. Schlame, M.; Towbin, J. A.; Heerdt, P. M.; Jehle, R.; DiMauro, S.; Blanck, T. J. Deficiency of tetralinoleoyl-cardiolipin in Barth syndrome. *Ann. Neurol.* **2002,** *51*, 634–663.
12. Hostetler, K. Y.; van den Bosch, H.; van Deenen, L. L. The mechanism of cardiolipin biosynthesis in liver mitochondria. *Biochim. Biophys. Acta* **1972,** *260*, 507–513.
13. Hirschberg, C. B.; Kennedy, E. P. Mechanism of the enzymatic synthesis of cardiolipin in *Escherichia coli*. *Proc. Natl. Acad. Sci. U.S.A.* **1972,** *69*, 648–651.
14. Schlame, M.; Rua, D.; Greenberg, M. L. The biosynthesis and functional role of cardiolipin. *Prog. Lipid Res.* **2000,** *39*, 257–288.

15. Schlame, M.; Brody, S.; Hostetler, K. Y. Mitochondrial cardiolipin in diverse eukaryotes. Comparison of biosynthetic reactions and molecular acyl species. *Eur. J. Biochem.* **1993,** *212*, 727–735.
16. Schlame, M.; Otten, D. Analysis of cardiolipin molecular species by high-performance liquid chromatography of its derivative 1,3-bisphosphatidyl-2-benzoyl-*sn*-glycerol dimethyl ester. *Anal. Biochem.* **1991**, *195*, 290–295.
17. Beckedorf, A. I.; Schaffer, C.; Messner, P.; Peter-Katalinic, J. Mapping and sequencing of cardiolipins from *Geobacillus stearothermophilus* NRS 2004/3a by positive and negative ion nano ESI-QTOF-MS and MS/MS. *J. Mass Spectrom.* **2002,** *37*, 1086–1094.
18. Lesnefsky, E. S.; Stoll, M. S. K.; Minkler, P. E.; Hoppel, C. L. Separation and quantitation of phospholipids and lysophospholipids by high-performance liquid chromatography. *Anal. Biochem.* **2000,** *285*, 246–254.
19. Peter-Katalinic, J.; Fischer, W. α-D-glucopyranosyl-, D-alanyl- and L-lysylcardiolipin from gram-positive bacteria: Analysis by fast bombardment mass spectrometry. *J. Lipid Res.* **1998,** *39*, 2286–2292.
20. Hsu, F.-F.; Turk, J.; Shi, Y.; Groisman, E. A. Characterization of acylphosphatidylglycerols from *Salmonella typhimurium* by tandem mass spectrometry with electrospray ionization. *J. Am. Soc. Mass Spectrom.* **2004,** *15*, 1–11.
21. Rhoades, E. R.; Hsu, F.-F.; Torrelles, J. B.; Turk J, Chatterjee, D.; Russell, D. G. Identification and macrophage-activating activity of glycolipids released from intracellular *Mycobacterium bovis* BCG. *Mol. Microbiol.* **2003,** *48*, 875–888.
22. Hsu, F.-F.; Turk, J. Characterization of phosphatidylinositol, phosphatidylinositol-4-phosphate, and phosphatidylinositol-4,5-bisphosphate by electrospray tandem mass spectrometry: A mechanistic study. *J. Am. Soc. Mass Spectrom.* **2000,** *11*, 986–999.
23. Hsu, F.-F.; Turk, J. Charge-driven fragmentation processes in diacyl glycerophosphatidic acids upon low-energy collisional activation. A mechanistic proposal. *J. Am. Soc. Mass Spectrom.* **2000,** *11*, 797–803.
24. Gilbin, D.; Hsu, F.-F.; Turk, J.; Gross, M. L. Mechanisms of characteristic phospholipid fragmentation, a theoretical study. *Proceedings of 52nd ASMS Conference on Mass Spectrometry and Allied Topics*; Nashville, TN, May, 2004.
25. Morrissey, B.; Tomas, M. C.; Mitchell, T. W.; Ung, A. T.; Pyne, S. G.; Blanksby, S. J. Negative ion phospholipid fragmentation: A mechanistic and regiochemical study. *Proceedings of 52nd ASMS Conference on Mass Spectrometry and Allied Topics*; Nashville, TN, May, 2004.
26. Hsu, F.-F.; Turk, J. Charge-driven and charge-remote fragmentation processes in diacyl glycerophosphoethanolamine upon low-energy collisional activation. A mechanistic proposal. *J. Am. Soc. Mass Spectrom.* **2000,** *11*, 892–899.
27. Henderson, T. O.; Glonek, T.; Myers, T. C. Phosphorus-31 nuclear magnetic resonance spectroscopy of phospholipids. *Biochemistry* **1974,** *13*, 623–628.
28. Kates, M.; Syz, J. Y.; Gosser, D.; Haines, T. H. pH-Dissociation characteristics of cardiolipin and its 2′-deoxy analog. *Lipids* **1993,** *28*, 877–882.